Eco-hydraulic modeling of the interactions between hydropeaking and river morphology

Davide Vanzo, Guido Zolezzi and Annunziato Siviglia

March 4, 2015

Corresponding Author:

Davide Vanzo - davide.vanzo@unitn.it

Dept of Civil, Environmental and Mechanical Engineering

University of Trento - ITALY.

Co-Authors details:

Guido Zolezzi - guido.zolezzi@unitn.it

Dept of Civil, Environmental and Mechanical Engineering

University of Trento - ITALY.

—

Annunziato Siviglia - siviglia@vaw.baug.ethz.ch

Laboratory of Hydraulics, Hydrology and Glaciology

Swiss Federal Institute of Technology, Zurich - SWITZERLAND.

This article has been accepted for publication and undergone full peer review but has not been through the copyediting, typesetting, pagination and proofreading process, which may lead to differences between this version and the Version of Record. Please cite this article as doi: 10.1002/eco.1647

Abstract

Hydropeaking related to hydropower operations produces adverse ecological effects that depend on its interaction with the channel morphology. A first quantitative attempt is proposed to investigate the eco-hydraulic response of different river morphologies to hydropeaking waves based on a 2D hydraulic modeling approach. Physical habitat diversity, macroinvertebrate drift and fish stranding, all relevant for hydropeaking, are quantitatively investigated with reference to realistic hydro-morphological conditions of regulated alpine streams. Habitat diversity and fish stranding have the strongest dependency on channel morphology and show nearly opposite behaviours with increasing morphological complexity. Braided reaches are the most resilient to hydropeaking offering the highest habitat diversity and very limited base-to-peak variation of macroinvertebrate drift, while alternate bars are extremely sensitive environments to drift and offer safer regions from stranding. Transitional morphologies between single- and multi-thread offer the best eco-hydraulic tradeoffs. The method allows to quantify to which extent same eco-hydraulic targets can be achieved by either morphological restorations or base flow increases: in transitional morphologies, identical reduction in reach-averaged stranding risk might be obtained by either halving the channel width or by a three-fold base flow increase; analogously, the same improvement in macroinvertebrate-fed areas can be achieved in a channel with alternating bars by either a three-fold base flow increase or by increasing 2.5 times the channel width. Such quantification of the eco-hydraulic effectiveness of complementary management strategies offers a powerful tool to support design of restoration measures in hydropeaking rivers.

1 Introduction

Hydropower generation is increasing at different paces worldwide because of its many advantages in comparison to other energy sources (e.g. Swiss Federal Office of Energy, 2013), despite concerns of potentially severe environmental effects on downstream water bodies, particularly in Alpine areas. Among the known impacts of hydropower generation, those associated with repeated artificial water level fluctuations downstream of hydropower plant releases pose particular challenges especially because their biophysical effects haven't been fully clarified yet (e.g.

Young et al., 2011; Harby and Noack, 2013). This complex process is known as hydropeaking and consists in a daily or even sub-daily repetition of small flood waves propagating downstream, with related artificially rapid fluctuations of water level, near-bed shear stress and flow velocity patterns. Hydropeaking has known multiple effects on fish communities (e.g. Vehanen et al., 2005; Young et al., 2011; Nagrodski et al., 2012) and macroinvertebrates (e.g. Bruno et al., 2013; Céréghino et al., 2004).

A lively debate has been growing in this last decade (e.g. Formann et al., 2007; Charmasson and Zinke, 2011) on the development of feasible mitigation measures for hydropeaking in order to promote an environmentally friendly hydropower development. Such mitigation measures are of essentially two types. *Operational* measures focus on the reduction of streamflow alterations at the source, like e.g. pump & storage systems or restrictions in turbine operation mode, while *constructional* measures (Person et al., 2013) focus on the management of the downstream river channel, like e.g. by promoting local river widening (Rohde et al., 2006) or more engineered morphological diversification (e.g. Meile et al., 2008).

Especially in Alpine areas, detection of the appropriate measures is often challenging: considering operational measures, one of the main advantages of hydropower production is the capability to follow almost instantly the fluctuations of electricity requests switching on/off turbines (Holland and Mansur, 2008). Therefore a reduction of electricity production can hardly be adopted as mitigation strategy. Nevertheless the variation of the released base flow, though implying economical losses for the producer, has been proposed as a feasible mitigation strategy for the ecological effects of hydropeaking (see e.g. Person et al., 2013). On the other hand, retention basins that could damp the hydropeaking waves often require large spaces that are hardly available at reasonable costs in productive Alpine valley floodplains.

Among morphological improvements, local widenings of channelized river reaches are increasingly carried out also in alpine areas where the availability of public land in valley floodplains is limited (Rohde et al., 2005). The rationale behind these measures is that giving "more room to the river" (Rohde et al., 2006) is normally expected to improve the health of river systems at least locally, because channel width represents a fundamental control on river mor-

phodynamics (e.g. Siviglia et al., 2008; Crosato and Mosselman, 2009). Widening is then expected to promote self-formed morphodynamics, leading to enhanced morphological diversity, and turn into more local hydraulic diversity (e.g. in water depth and flow velocity patterns). Such hydro-morphological diversity is often expected to give rise to improved ecosystem health (e.g. Elosegi et al., 2010).

When the target river reach is subjected to hydropeaking, however, evidence from monitoring of river widening programs has shown little ecological improvements in restored reaches despite the increase in morphological diversity (e.g. Muhar et al., 2007). In a recent assessment of hydropeaking mitigation measures, Person et al. (2013) indicate that increasing morphological complexity generally offers the best habitat condition, but they also suggest that at the same time this condition may maximize the stranding risk for fish species. The review of Harby and Noack (2013) points out the relevance of the interactions among hydropeaking and morphological diversity, further remarking the relevance of their better understanding as well as that such assessment is difficult also because often site-specific. This interaction has been so far only qualitatively predicted, i.e. within a hydro-morphological alteration space originally inspired by Baumann et al. (2012), which has the merit of trying to overcome the site-specificity of the problem. Figure 1 shows how the best expected ecological response (blue region) should occur in the combination of high morphological complexity and vanishing hydropeaking intensity. Moreover it indicates that ecological improvements can be reached both through "horizontal" strategies, which act on morphological complexity, as well as through "vertical" strategies, which modify the hydropeaking intensity, or through a combination of both (e.g. "diagonal" strategies).

In the present paper we aim at quantitatively exploring ecologically-relevant hydraulic interactions between different hydropeaking scenarios and different channel morphologies, through the use of 2D hydraulic modeling. More specifically we aim at developing a modeling approach able to: (i) quantify two-dimensional eco-hydraulic effects of different channel morphologies on the propagation of hydropeaking waves of different intensities; (ii) compare the response of different Ecologically-Relevant Hydraulic Parameters (hereinafter EHRPs) to changes in

the morphological pattern of the riverbed and in the base flow; (iii) support the analysis of tradeoffs between operational (i.e. increase in base flow) and constructional (i.e. channel widening/narrowing) mitigation measures. The results allow to quantify the variability of well-recognized, Ecologically-Relevant Hydraulic Parameters when "horizontal", "vertical", or "diagonal" mitigation measures (Figure 1) are implemented on a hydropeaked river reach. Though not pretending to achieve a complete generality, we try to cover a representative set of combinations of realistic hydropeaking scenarios and realistic morphological patterns that can be found in alpine areas.

The potential of hydraulic numerical modeling has been already exploited in recent years with the aim of evaluating reach scale hydro-ecological effects, also in relation to hydropeaking. Hauer et al. (2013) used a 1D numerical model to investigate the longitudinal damping of hydropeaking waves due to the characteristics of the downstream channel, while Gostner et al. (2013b) focus on the quantification of morphological variability at different flow discharges in some specific sites using a 2D model. Casas-Mulet et al. (2014a) test and explore the capability of a 1D numerical model to quantify fish-stranding areas on rivers subject to hydropeaking. Differently from previous studies, our focus here is on modeling the interaction between reach self-formed morphology and hydropeaking events at reach scale through a 2D depth averaged numerical model.

2 Methods

The modeling approach to investigate the eco-hydraulic interaction between hydropeaking and channel morphology can be summarized in three main steps: firstly we set a suite of hydropeaking scenarios and river bed patterns (Sections 2.1, 2.2 and 2.3), which represent the inputs for the numerical simulations; secondly we perform the numerical simulations (Section 2.4) using GIAMT2D, a 2D (x-y) shallow-water numerical model (Siviglia et al., 2013); thirdly the hydraulic numerical variables (e.g. flow velocity, water depth) resulting from the simulations are summarized in a single parameter which accounts for a specific ecological effect (Section 2.5).

In more detail, a series of 36 numerical runs under steady flow conditions have been performed, simulating three different hydropeaking scenarios in combination with six different channel morphologies. All the simulated hydropeaking-morphological combinations have been designed with the aim to reproduce realistic conditions of medium-large alpine river reaches subject to hydropeaking. A full generalization, and a rigorous scaling approach able to quantitatively consider all possible real configurations is out of the scope of the present work.

The research design has therefore foreseen three basic choices, which respectively set the input discharge, the topographical domain and the outcomes of the hydraulic model simulations that are relevant for the scope of the work. The input discharge is associated with the peak and base values of a representative hydropeaking scenario. The topographical domain is constructed starting from six different experimental channel morphologies obtained in mobile-bed flume experiments by Garcia Lugo et al. (2013). In particular, the different channel morphologies are obtained by varying the externally imposed channel width and keeping the same flow rate, sediment size and longitudinal slope; they cover a suite of representative channel patterns that include nearly flat bed without relevant bedforms, alternate bars, wandering and braiding configurations.

The simulation outcomes are analysed in terms of a suite of quantifiable Ecologically-Relevant Hydraulic Parameters (Section 2.5) assumed as representative of three eco-hydraulic phenomena chosen because they are of typical concern under hydropeaking conditions: physical habitat or hydro-morphological diversity, macroinvertebrate drift and fish stranding. Such ERHPs allow to measure the effects of hydropeaking interaction with different channel morphologies, hence to quantitatively compare different configurations in the hydro-morphological alteration space. Results are then analysed in terms of the spatial distributions of each ERHP at the reach scale and discussed comparatively.

2.1 Hydropeaking Events

For the sake of simplicity, we consider a single hydropeaking event schematized as a rectangular wave, characterized by a base discharge Q_{base} and a peak discharge Q_{peak} (Figure 2). In real

cases the base flow could correspond to the minimum environmental flow, constantly released from the upstream dam, while the peak discharge is obtained by adding the discharge released by the hydropower plant (Q_{prod}, for electricity production) to the base flow. For the sake of simplification, we adopt an hydropeaking wave as in the "worst" possible ecological scenario, whereby discharge instantaneously varies from base to peak and viceversa.

Three different hydropeaking patterns (A, B and C) are considered in the study (Table 1): they are built by varying the base flow Q_{base} and keeping the same discharge value used for electricity production Q_{prod}. The selected range of the ratio Q_{peak}/Q_{base} can be often found in alpine and piedmont scenarios. Changes in Q_{base} may correspond to different imposed environmental flows from the dam or in the subcatchments that contribute in the reach located between the dam and the water release section.

2.2 Channel Morphologies

The bed morphologies used in the present work are based on detailed topographic scans of simulated river bed patterns in a series of laboratory flume experiments performed by Garcia Lugo et al. (2013). Namely, the considered topographies result from six experiments in a mobile bed laboratory flume with fixed banks and the same values of water discharge, initial mean bed slope and sediment size. Each experiment differs only for the imposed channel width (ranging from 0.15 m to 1.5 m). The system freely develops from an initial flat bed towards a morphodynamic equilibrium state, characterized by constantly changing bed morphologies whose configuration is statistically different among different runs. Experiments show how, increasing only the available channel width, the bottom pattern shifts from flat bed (narrow channel) to braiding network (wide channels), passing through transitional configurations characterized by alternate bars and wandering morphologies. These original flume reaches are 14.5 m long and the provided scans of equilibrium pattern have a spatial resolution of 50 mm and 5 mm in longitudinal and transverse direction respectively. Then a total of 290 cross sections are available for each configuration.

In order to get realistic bathymetries resembling to alpine river reaches we have scaled the

flume topographies using a simple geometrical similarity. Therefore the bottom scans of the six original experiments and the mean sediment grain size have been multiplied by a factor $\lambda = 100$. The upscaled morphologies that have been used in our analysis thus span a channel width range between ($15\ m \div 150\ m$), are 1450 m long and have a uniform grain size ($D_s \approx 0.1\ m$). The main geometrical characteristics of the adopted morphologies are given in Table 1. In particular, morphology 1 has almost flat bed, 2 and 3 show an alternate bar pattern with different bar amplitude (larger for case 3) while pattern 4 is characterized by a transitional wandering channel. Finally, morphologies 5 and 6 show different braiding patterns. Figure 3 reports a planar view (x-y, with magnified y axis for the sake of clearer visualization) and one illustrative cross section (y-z) of the channel for three sample morphologies: flat bed (1), alternate bars (3) and braiding (5). Figure 3 clearly shows the key role of the channel width in driving different morphological patterns.

2.3 Hydro-Morphological Configurations

The designed three hydropower production patterns (A, B, C in Table 1) and six self-formed morphological patterns (from 1 to 6 in Table 1) provide 18 possible configurations that can be visualized in the hydro-morphological alteration space of Figure 1. In this diagram unaltered hydro-morphological configurations are those laying close to axis origin, while hydrological (y axis) and morphological (x axis) alterations can be thought to increase when moving away from the origin. We parameterized hydrological alteration, i.e. hydropeaking intensity, through the ratio Q_{peak}/Q_{base}, which therefore decreases moving downwards; note that this corresponds to increase base (or environmental) flow. On the other hand, morphological complexity is parameterized with the widening ratio W/W_0 computed with respect to smallest width value of all the upscaled morphologies ($W_0 = 15\ m$) and it increases when moving from right to left. For the sake of clarity, each configuration is labelled in the form "WK", where W denotes the hydropeaking pattern (A, B o C in Table 1), K is the analysed upscaled morphology (from 1 to 6, Table 1). For example, A3 corresponds to release pattern A ($Q_{peak} = 50\ m^3/s$, $Q_{base} = 5\ m^3/s$) and morphology 3 (alternate bars).

Each hydromorphological configuration is also characterized by a longitudinal reach-averaged bed slope that has been chosen equal to 0.003 m/m, a realistic value for alpine and piedmont river reaches with channel width in the range (15 $m \div 150$ m). It is worth mentioning that our hydromorphological configurations have been set up with the aim of being realistic representations of hydropower-regulated alpine/piedmont streams: therefore the upscaled experimental scans are used only as topographic representation of different channel patterns. For the same reason, neither the chosen slope nor the base/peak discharge values need to match the corresponding values in the laboratory experiments. In other words, the channel bed morphology and the chosen hydropeaking discharges are independent variables. This would not be the case if aiming at closely reproducing the experimental runs with the numerical hydraulic model, when the discharge value is the channel-forming one, i.e. the one that generates the examined morphologies.

2.4 Hydraulic Modeling

Hydraulic simulations has been conducted with GIAMT2D (Siviglia et al., 2013), a non-stationary 2D (x-y) shallow water numerical model build on unstructured triangular grids. A robust wet-and-dry algorithm is implemented, allowing the correct simulation of emerging topography. The different computational domains are built on the upscaled bathymetries of lab experiments (see Table 1) and have number of cells ranging from 94810 (morphology 1) to 163528 (morphology 6) with mean cell area equal to 0.4 m^2 and 1.6 m^2, respectively. For the reasons explained in Section 2.3, there is no need for a calibration of the roughness coefficient with water level data from the laboratory runs, and therefore for all the numerical runs we set bed roughness (Strickler coefficient Ks) equal to 30 $m^{1/3}s^{-1}$. The value is estimated from the well-known Strickler formula $K_s = 21.1/D_s^{1/6}$ ($K_s = 1/n$, where n is the Manning coefficient), where D_s is the upscaled mean grain size. Simulations are performed with fixed bed, imposing a constant inflow discharge at upstream boundary (see data in Table 1) and uniform flow as downstream boundary condition. Each of the 36 numerical runs (18 configurations for 2 discharge stages) reach steady conditions roughly within 1-2 hours of simulated time. The simulated local values

of flow depth and velocity are then statistically analysed over all the wet cells.

2.5 Ecologically Relevant Hydraulic Parameters

Three relevant eco-hydraulic effects have been considered: the variation of physical habitat diversity between high and low discharge stages (e.g. Gostner et al., 2013b), the catastrophic drift of benthic organisms during the rising limb (e.g. Bruno et al., 2010, 2013) and the fish stranding during the rapid recession phases (e.g. Halleraker et al., 2003). Each of these ecological effect has been associated with one measurable Ecologically-Relevant Hydraulic Parameters. It must be noted that the choice of these three ERHPs can not be considered as exhaustive: the investigated ecological effects are driven also by other biotic and physical parameters that are not considered here, as rising and falling discharge rates (e.g. Nagrodski et al., 2012).

As quantitative indicators (ERHP) related to each examined ecological effect, we choose: i) a measure of spatial heterogeneity of water depth and velocity, which reflects habitat diversity availability; ii) the magnitude of the near-bed shear stress as primary cause of macroinvertebrate drift; and iii) the variation of wetted area between high and low stage which is associated with fish stranding. It is worth mentioning that different choices for the velocity are available in order to compute the first and the second ERHP. Among them one can choose the velocity U along the longitudinal direction or the magnitude $|U| = \sqrt{U^2+V^2}$ where V is the velocity along the transversal direction. Our analyses, not presented here, show that the results are slightly affected by this choice. Therefore we decide to compute the two ERHPs using U because this would allow an immediate comparison with the data obtained from one-dimensional modeling approaches.

2.5.1 Hydro-Morphological Index of Diversity

Habitat heterogeneity has been recognized to be a key-point for ecosystem integrity (e.g. Elosegi et al., 2010) and the variability of water depth and flow velocity distributions reflects the river spatial complexity and heterogeneity. Gostner et al. (2013a) developed an Hydro-Morphological Index of Diversity (HMID) at reach scale based on the variability of flow velocity and water

depth spatial statistic distributions for a given flow discharge. The HMID index reads

$$HMID = \left(1 + \frac{\sigma_U}{\mu_U}\right)^2 \cdot \left(1 + \frac{\sigma_D}{\mu_D}\right)^2, \quad (1)$$

where σ_U and μ_U are depth-averaged flow velocity in longitudinal direction (U) standard deviation and mean value, respectively. Similarly, σ_D and μ_D are water depth (D) standard deviation and mean value, respectively. Ratio σ/μ is the coefficient of variation (CV) and it represents the extent of variability in relation to the mean value of the distribution.

For simple morphologies (i.e. straight channelized reach with almost flat bed) flow velocity and water depth tend to have uniform values ($\sigma \to 0$), so in Equation (1) HMID is a small value close to one. On the other hand, high morphological complexity causes heterogeneous distributions of the hydraulic variable (larger ratios σ/μ), with a consequent increase of the HMID value. Gostner et al. (2013a) tune the HMID values for a set of representative Swiss pre-alpine sites and identify three hydro-morphological categories:

1. $HMID < 5$: occurs in case of channelized and morphologically heavily altered reaches;
2. $5 < HMID < 9$: transitional range from heavily modified to almost natural morphology;
3. $HMID > 9$: morphologically natural reaches.

2.5.2 Macroinvertebrate Drift

Macroinvertebrate communities are naturally subjected to catastrophic and behavioural drift in unaltered flow regime reaches but this process has been shown increasing in presence of hydropeaking (e.g. Bruno et al., 2010; Céréghino et al., 2004). Being the flow velocity close to the bottom the driver of macroinvertebrate drift, we evaluate it in terms of bottom shear stress (τ). Choosing the Strickler parametrization for roughness, the bottom shear stress in each cell is evaluated as:

$$\tau = \rho g \frac{U^2}{K_s^2 D^{1/3}} \quad \left[\frac{N}{m^2}\right], \quad (2)$$

where ρ is water density and g gravity acceleration.

Even though different macroinvertebrate species are characterized by different drift resistance depending also on their ability to hiding and sheltering, we assume a unique threshold value for the onset of all macroinvertebrate drift as presented by Hauer et al. (2012). This value is set to $\tau_{drift} = 10\ N/m^2$. The threshold approach is useful to quantitatively discriminates two opposite behaviour for macroinvertebrate communities: with low bottom flow velocity ($\tau < \tau_{drift}$) individuals are able to settle down and colonize the river bed, while with high flow velocity ($\tau > \tau_{drift}$) they tend to be drifted away. From the food chain perspective, the former case can be defined as *sink* behaviour, representing areas with macroinvertebrate biomass accumulation, while the latter case can be defined as *source* behaviour, being the drifted biomass available for fish feeding.

We have chosen to evaluate the shear stress only in the reach bed portion which is submerged both at high and low stages, because daily or even subdaily emergence of bedforms can not allow the settling of stable macroinvertebrate communities.

2.5.3 Fish Stranding

Fish stranding could be a serious hazard for fish communities (especially for early-life stages) and it may occur under different circumstances. Under hydropeaking conditions rapid flow fluctuations may alternately wet and dry river bed areas (Nagrodski et al., 2012). During high flow stages fishes can move and occupy available lateral shallow water regions for feeding, sheltering and spawning but, depending on extension of dried areas and rate of change of water level, they can be stranded during the falling limb of hydropeaking event.

In this work we take into account only the variation of wetted area during an hydropeaking event as ERHP, not considering the water level rate of change. Moreover it is worth noting that the daily drying of spawning areas, which can increase eggs and juvenile fish mortality, strongly depends on the magnitude of the variation of wetted area rather than water level rate of change (e.g. Casas-Mulet et al., 2014b).

The variation ΔA_w of wetted area A_w during hydropeaking event is evaluated according to

the Swiss protocol (Baumann et al., 2012) as

$$\Delta A_w = \frac{A_w^{peak} - A_w^{base}}{A_w^{peak}} \cdot 100 \ [\%], \tag{3}$$

where the superscript indicates the discharge stage (peak or base). Referring to the Swiss protocol, cross sections with $\Delta A_w < 30\%$ can be considered in "good" status, so with low risk of stranding.

Wetted area variation has to be evaluated locally at cross section scale, as suggested also by Baumann et al. (2012). Hence ΔA_w (Equation 3) is computed slicing each river reach (1450 m long) along the transversal direction. We use slices 5 meters wide obtaining a total of 290 subareas. For each subarea we evaluated the variation of wetted area (calculated with Equation 3) and compute the statistics over the 290 subareas of each reach.

2.5.4 Overall Comparison of Different ERHPs

In order to set up a comparative analysis among all the three examined eco-hydraulic phenomena a unique metric is needed for each ERHP, able to account for the difference between base and peak flow conditions. We have therefore chosen the loss of the HMID from base to peak for habitat diversity, the percentage loss of macroinvertebrate sink area for drift and the percentage of wetted area in good status in relation to the adopted fish stranding criterion. Such comparison is deliberately simplified and it assumes that intermittent hydropeaking waves always fluctuate between the same two discharge values.

Furthermore, an ensemble measure of the overall eco-hydraulic response of each analysed channel morphology to hydropeaks with different base flow conditions has been developed. Conceptually such measure is based on recognizing that the continuous shift between base and peak flows determines an extremely harsh environment. The worst of the two states, in ecological terms, has to be viewed as the most limiting state and therefore the most representative of the system eco-hydraulics conditions on long terms.

More specifically, for each of the 18 examined configurations, the following three steps have been followed. i) We have sought a normalized score within the same range 1 to 4 (1: worst; 4:

best) for each of the three eco-hydraulic phenomena, to ensure inter-phenomena comparability. ii) For the case of habitat diversity and invertebrate drift, we have assigned such score to every combination, both for peak and for base flow, and then we have chosen the lowest value, corresponding to the most limiting condition, as the unique representative of each combination. In the case of stranding risk, a unique score could be immediately given, being the phenomenon already defined by both base and peak flow. iii) The ensemble eco-hydraulic response for each of the 18 examined hydromorphological configuration was evaluated as the average of the representative scores for habitat diversity, drift and stranding risk. Under step i), for every ERHP, the maximum score (4) has been assigned to every combination in the best eco-hydraulic status, i.e. every combination found in the blue areas of the diagram representing the ERHP behaviour in the hydromorphological space of Figure 1, and viceversa for the minimum score (1), which has been assigned to every combination found in the red parts of the same diagrams. Intermediate scores have been given to combinations found in the green and yellow areas on the basis of linear interpolation between the maximum and minimum values.

3 Results

The results of numerical simulations are discussed in term of reach-scale metrics based on spatial statistics of the selected ERHPs. This allow us to highlight and quantify the role of reach-scale morphology in defining ERHP distributions. We first discuss the numerical results in terms of the fundamental hydraulic quantities (flow velocity and water depth) and use this as a reference to present the results related to each ERHP.

3.1 Spatial Distribution of Flow Depth and Velocity

The statistical distributions of simulated water depth and longitudinal flow velocity are represented in the form of a box and whiskers plot in Figure 4. The plots show the distribution for the production pattern A ($Q_{peak}/Q_{base} = 10$), which corresponds to the strongest hydropeaking intensity among the three examined in the present work, and the six morphologies (1 to 6).

Results are displayed for base (Figure 4a,c) and peak flow (Figure 4b,d).

As it can be expected, the median values of the depth and velocity distributions (center line of each box) generally increase from base to peak flow and decrease for increasing morphological complexity (i.e. by increasing widening ratio, from A1 to A6), though those relations are non-linear and characterized by the presence of thresholds where different behaviours can be detected. For instance, median values of the depth and velocity distributions almost do not change when morphological complexity increases in the case of the multi-thread morphological configurations (A4-A5-A6). In these channel morphologies median values also show very little increase when passing from base (Figure 4a,c) to peak flow conditions (Figure 4b,d), compared with "simpler" morphologies corresponding to nearly flat bed without bedforms or alternate bars (A1-A2-A3).

Besides changes in median values among the examined configurations, for the purpose of the present work the variability of local flow depth and velocity values is particularly important, because they reflect the hydraulic heterogeneity of local conditions for a given hydro-morphological configuration. In Figure 4 the overall spatial variability is represented by the extension of the box (interquartile range) and of the whiskers for the different morphologies. For the same discharge value, water depth is highly variable in complex morphological configurations (A4-A5-A6), especially in comparison with the simpler morphological patterns (A1-A2-A3) (Figure 4a,b). The same behaviour does not apply for flow velocity, for which the variability is comparable among the examined morphological categories, and differences are much less evident.

The invariance of the median values from base to peak discharge and the higher variability of the local values may be related with the higher resilience of the morphologically complex systems (A4-A5-A6) to discharge variations and matches the common perception that greater morphological complexity should ensure higher ecological functionalities (e.g. Elosegi et al., 2010).

3.2 Hydro-Morphological Index of Diversity

As a quantitative, species-independent quantification of the physical habitat variability among the examined hydro-morphological configurations we have computed the hydro-morphological index of diversity HMID (Section 2.5.1). In Figure 5 the HMID value is plotted against the six considered widening ratios W/W_0 that have been related with the considered morphologies. Each continuos line refers to a different discharge, namely corresponding to the "base" and "peak" values under the three considered hydropeaking scenarios (Table 1).

The dependency of the HMID on the widening ratio is clearly non-linear and is qualitatively similar for all the chosen hydropeaking patterns. Regardless of the chosen discharge value, the HMID invariably increases with morphological complexity. For instance, the Bbase series refer to $Q = 10\ m^3/s$ and show low HMID values ($HMID < 5$) for the two simplest morphologies characterized by nearly flat bed or alternate bars ($W/W_0 = 1, 1.33$, right side of the plot). For higher widening ratios the HMID value grows more rapidly and attains moderate values ($5 < HMID < 9$) for the alternate bars configuration associated with $W/W_0 = 2$. The growth of the HMID with the widening ratio is eventually reduced and tends to stop around an approximately constant value of $HMID \approx 20$ for the most complex, multi-thread morphologies ($W/W_0 = 5.33, 6.66, 10$). This means that channel widening beyond $W/W_0 = 5.33$ cannot determine further increase of the diversity of physical habitat conditions, measured through the HMID.

Nonlinearity is also evident in the effect of flow discharge, because the vertical spacings between the curves referring to base flow are much larger compared to those at peak flows (Figure 5). Under peak flow conditions (A,B,Cpeak) the bed morphologies are almost fully submerged, and the different trends are almost overlapped. This suggests that the peak discharges associated with nearly complete wetting conditions of the active channel bed do not significantly affect the HMID. It turns out that it is basically dependent on channel morphology under these conditions.

Comparing the values from Figure 5 with the HMID categories proposed by Gostner et al. (2013a) it is possible to highlight that the braiding configurations ($W/W_0 = 5.33, 6.66, 10$) lay

always in category 3 ($HMID > 9$, morphologically natural) while the simple morphologies ($W/W_0 = 1$ - flat bed and $W/W_0 = 1.33$ - small alternate bars) are always within category 1, no matter the choice of discharge pattern. On the other hand, for the morphology number 3 ($W/W_0 = 2$ - alternate bars) the HMID values lay in different categories depending on the chosen hydropeaking series (so for different discharge stages).

The quantitative information reported in Figure 5 can be used to build the hydro-morphological alteration space as in Figure 1. Thus we can plot the quali-quantitative spaces in Figure 6, which show the hydro-morphological tradeoffs for HMID index. Black dots represent the 18 configurations, labelled (in blue) with the obtained value of HMID. The space is divided in three regions by the locus of points having HMID equal to 9 and 5, qualitatively defined by linear interpolation of values in Figure 5. With this view, blue region gathers configurations with $HMID > 9$, green area with $5 < HMID < 9$ and red region with $HMID < 5$. Figure 6a refers to base flow while Figure 6b to peak flow conditions. The HMID is strongly dependent on morphology (thresholds are predominantly vertical) while it smoothly changes with increases in the base flow (Figure 6a). Moreover, the comparing between the base and peak configurations show a sensible temporal variability of HMID for morphologies between transitional and alternate bars (W/W_0 =2 to 4), while the HMID almost shows no base-to-peak change of class for the other channel morphologies (Figure 6a,b).

3.3 Macroinvertebrate Drift

For this ERHP we analysed the statistical distributions focusing both on the variation from base to peak conditions (temporal variability) and on the variation linked to different morphologies (spatial variability). In Figure 7a mean values of the bottom shear stress are plotted for six widening ratios W/W_0 corresponding to the different morphologies. The data series represent the different release patterns (A,B and C) both for peak and base flow. Mean values are useful to understand general trends for this ERHP: the bottom shear stress decreases non linearly as the widening ratio increases. It is worth noting how, for more complex morphologies ($W/W_0 = 5.33, 6.66, 10$), the ERHP tends to flatten, suggesting the type of self-formed

morphology strongly influence ERHP's distribution.

We then apply the hydraulic threshold criteria ($\tau_{drift} = 10\,N/m^2$, Hauer et al., 2012) and plot the percentage of area with bottom shear stress lower than the drift threshold (τ_{drift}). In Figure 7b is shown how increasing the widening ratio, so varying the reach morphology, makes mean shear stress decreasing, with reach that tends invariantly to increase the areas where macroinvertebrate communities can settle (shear stress under the threshold, sink behaviour). However in Figure 7b is possible to quantify how the most relevant differences of the series occur for low discharge stages (base discharge) and simple morphologies ($W/W_0 = 1, 1.33, 2$). On the other hand, once bed morphologies are almost fully submerged (peak discharge stages) there are no relevant differences between series A, B and C.

Figure 8 reports the hydro-morphological alteration space for the macroinvertebrate drift (with the values of Figure 7b) for base flow (Figure 8a) and peak flow (Figure 8b) conditions. Blue labels are the percentages of area with sink behaviour ($\tau < \tau_{drift}$). Blue regions represent configurations with dominant (more than 75%) settling of macroinvertebrate communities while, on the opposite, red regions represent scenarios dominated by macroinvertebrate drifting. At base flow condition (Figure 8a), the sink/source behaviour is determined by both base flow variability (i.e. Q_{peak}/Q_{base}) and by channel pattern for the less complex morphologies (small widening ratios). On the other hand, channel morphology becomes the dominant control on the sink/source behaviour, compared to base flow variability, when moving to braided systems (left part of the space). Moreover, in the case of peak flow, we observe a strong reduction of sink behaviour (absent blue region).

3.4 Fish Stranding

Results for the mean wetted area variation, plotted versus the widening ratio W/W_0 are given in Figure 9. As first consideration the trend of this ERHP is depending on the type of reach morphology with a great increment passing from alternate bar pattern ($W/W_0 = 2$) to braiding system ($W/W_0 = 5.33$) but the variation keeps increasing also with an established braiding system (left part of the plot, $W/W_0 = 6.66, 10$).

In order to highlight the percentage of area that can be considered in a good status (so with low risk of stranding, according to Baumann et al., 2012), we show on Figure 10c the area in a good status (with wetted area variation lower than 30%) versus the widening ratio W/W_0. The hydro-morphological alteration space for stranding risk in Figure 10c has been obtained firstly by determining, for each of the 18 hydropeaking-morphology configurations, the percentage of area satisfying the criteria $\Delta A_w < 30\%$ (blue labels in Figure 10c). Afterwards, the same procedure leading i.e., from Figure 7b to Figure 8, has been adopted. The three extrapolated threshold curves represent the locus of points with 25%, 50% and 75% of wetted areas in a good status, respectively. The thresholds divide the space into 4 regions with an increasing risk of stranding moving from blue to red region.

In Figure 10c it can be easily seen that the area with low stranding risk invariably decreases when the widening ratio (channel width) increases, showing a non-linear trend associated to the different effects of the reach morphology. Overall, stranding risk is dependent both on reach morphology and on hydropeaking intensity. However, it is almost independent from flow discharge in morphologies with a less degree of morphological complexity (i.e. $W/W_0 = 1, 1.33, 2$, right part of the space). Opposite to the ensemble ecological response suggested by the initial Figure 1, this ERHP reveals the worst ecological situation (i.e. highest stranding risk) in correspondence of high morphological complexity ($W/W_0 = 5.33, 6.66, 10$).

3.5 Comparative Analysis of ERHPs Response to Hydropeaking for Different Morphologies

The present work has focused on the analysis of one single hydropeaking wave. In real cases, the presence of hydropeaking intrinsically implies that the affected river reach is subject to a repeated daily or sub-daily switch from base to peak flow conditions, and may therefore be viewed as "two rivers in one", as recently pointed out by Jones (2014). The inherent intermittency of the hydropeaking phenomenon is accounted for in Figures 10 and 11 that are an attempt to synthetically quantify the hydropeaking effect of for each ERHP separately (Figure 10) and jointly (Figure 11).

Figure 10 reports the quantitative behaviour of habitat diversity loss (Figure 10a), of drift sink area loss (Figure 10b) and of the percentage of wet area in good status with respect to stranding risk (Figure 10c), in the form of the hydromorphological space introduced in Figure 1. Each of these diagrams is representative of the response of each ERHP to one hydropeaking wave as a whole, while Figures 6a,b and 8a,b refer to the behaviour of the ERHP under either base or peak flow conditions.

Comparing Figure 6, 8 and 10 allows to quantify how different is the role of hydropeaking for the three phenomena of drift, stranding and habitat diversity across the range of examined bed morphologies. A prevalent horizontal gradient from red to blue areas in the hydromorphological spaces indicates a dominant morphological control on the ERHP behaviour, regardless of the hydropeaking intensity (or base flow increase). This is the case of hydro-morphological diversity at base (Figure 6a) and peak (Figure 6b) flow conditions and of the percentage of wet areas in good status with respect to the stranding risk (Figure 10c).

In contrast, the base to peak loss of habitat diversity, expressed in Figure 10a through the HMID difference between base and peak flow conditions, seems to be fundamentally controlled by hydropeaking intensity almost regardless of the channel pattern. The location of the red region around $W/W_0 = 5.33$ also suggests that transitional morphologies between single and multi-thread are the most sensitive to intense hydropeaking because they determine a higher loss of hydromorphological diversity compared both to alternate bars and braided channel patterns for a given hydropeaking intensity. An exception to such behaviour is related to the simplest morphological configurations (widening ratio smaller than 1.33), where the loss of diversity is much more limited and almost independent from the hydropeaking intensity, though the limiting factor here is the low absolute HMID value under base flow condition, due to the poorly developed bed topography.

The response of macroinvertebrate sink areas does not show clear trends with either channel morphology or hydropeaking intensity like the other two ERHPs do, with the two hydromorphological controls being more balanced and nonlinear trends being more distinctive of the ERHP at both base and high flow, and also of its base-to-peak loss. Such loss of sink areas is

strongly sensitive to hydropeaking in alternate-bar channel patterns, and is nearly unaffected by base flow increase for wandering or braided morphologies, which correspond to an almost constant loss of 40% (nearly homogeneously green left portion of Figure 10b).

The performance of each ERHP is finally aggregated in Figure 11, as described in Section 2.5.4, to obtain an overall eco-hydraulic comparison among the examined 18 hydropeaking - channel morphology combinations. Figure 11 suggests how morphologies from wandering to low braiding seem to provide the optimal eco-hydraulic conditions, while a further increase of the braiding intensity corresponds to a reduction of the representative score because of the high associated increase in stranding risk. The lowest scores are found for widening ratios corresponding to alternate bars or smaller. The strongest variability in the eco-hydraulic response to hydropeaking is found when the river pattern transitions from alternate bars to wandering. Such response does not seem to vary considerably in the range of examined hydropeaking intensities, from about 1:3 to 1:10.

4 Discussion

4.1 Morphological Controls on Hydropeaking Effects

The proposed modeling approach allows to highlight trends in the eco-hydraulic response of a river reach along a gradient of different channel morphologies, from almost flat bed to braiding. Overall the eco-hydraulic response shows a high degree of nonlinearities in behaviour, in qualitative agreement with the findings of Hauer et al. (2014).

Braided reaches appear as the most resilient to hydropeaking in terms of the absolute high availability of habitat diversity (HMID>9), of the very limited loss of invertebrates sink areas and of habitat diversity, especially if compared to wandering morphologies. The major concern with a braided river reach subject to hydropeaking lies in its high risk of stranding. Braided river reaches are very uncommon in the contemporary landscape of hydropower-regulated river systems, at least in the alpine region of Europe. Among the few ones recognized as "near-natural", the braided Tagliamento River (Bertoldi et al., 2009) is subjected to hydropeaking

characterized by a rather limited intensity in all seasons of the year, which is not causing any relevant threat to the fish population.

When moving to single-thread morphologies, alternate bars are predicted to be extremely sensitive environment to macroinvertebrate drift, to offer safer regions from stranding and also are not affected by relevant diversity loss, though their diversity is never particularly valuable in ecological terms (HMID usually < 9). In a recent study, Hauer et al. (2014) analysed the stranding risk associated with different types of gravel bars, by combining information on peak-to-base change in wetted area, on shallow habitat availability and on substrate grain size composition to develop and apply a conceptual stranding risk model. They simulated almost identical hydropeaking intensities (1:3, 1:5 and 1:10) to the present analysis, occurring over several sites with different bar morphologies in regulated Austrian rivers. The outcome of the stranding risk model of Hauer et al. (2014) highlights a qualitatively analogous contrasting effect of gravel bar morphology with respect to the one emerging from the present analysis: simpler morphologies, found in more regulated reaches, featured the smallest reduction in wetted area, coherently with the blue region in our Figure 10c. However the same morphologies are also characterized by the absence of minimum suitable habitats, as it also emerges from our Figure 6a,b at both base and peak flow.

Moreover, Hauer et al. (2014) emphasize the role of bar morphology on stranding risk. They point out a difference in behaviour between point bars, which occur at the inner side of river bends, alternate bars, which develop in straightened river reaches, and mid-channel bars. Point bars feature a smaller variability in wetted area compared to alternate bars, and thus display less sensitivity to hydropeaking, in some way analogously to mid-channel bars. The point bar tails are characterized by smaller-scale topographical structures that create suitable habitats at both peak and base flow and also the overall morphology of the two types of bars is quite different. In our work, widening determines an analogous increasing morphological complexity, with less regular bar pattern and superimposed smaller scale heterogeneities (Figure 3). For instance, when moving from $W/W_0 = 2$ to $W/W_0 = 5.33$, secondary channels develop alongside alternate bars and progressively become more relevant in the whole reach morphology, before this

becomes fully braided.

The outcomes of our study suggests that transitional morphologies between single and multi-thread offer the most interesting and less trivial behaviour, because they offer the best tradeoff between sink area loss and percentage of dewatering-safe areas (see the corresponding green areas in Figure 10b) among the non-trivial morphological configurations. This is reflected by the overall eco-hydraulic "optimum" as it emerges from the score reported in Figure 11, which has been obtained by averaging each ERHP-specific score. Interestingly, such result is only morphology-dependent and does not seem to be affected by hydropeaking intensity. The relevant role of the transitional morphologies is coherent with the findings of Person et al. (2013), who performed a comparative analysis of several hydropeaking mitigation measures. Person et al. (2013) noted that "braided reaches provided the richest in-stream structure", i.e. habitat diversity and availability, though "braided" there refers to a reach with a main channel and one single secondary, smaller channel, separated by a gravel bar with superimposed smaller-scale irregularities, thus resembling an actually wandering or transitional morphology. While Hauer et al. (2014) indicate that no "optimal" river topography for hydropeaking mitigation could be found among the examined 16 bar reaches in their study, our analysis suggest that at least the best tradeoff, if not optimal conditions, are actually provided by such transitional patterns. This type of channel morphology is increasingly dominating the regulated fluvial landscape since the last decades, at least in Europe and in other pre-alpine contexts in the industrialized world (e.g. Surian and Rinaldi, 2003; Habersack and Piegay, 2007), because of channel adjustments of formerly braided reaches caused by altered flow and sediment regimes, as well as by gravel mining. The occurrence of hydropeaking over transitional channel morphologies may therefore be already frequent in alpine areas with strong hydropower development, may characterize morphologically restored (locally widened) river reaches and may also increasingly occur in the future in alpine-piedmont areas with yet unexploited hydropower potential.

The topographic differences between the different types of bars observed by Hauer et al. (2014) are qualitatively consistent with theoretical and experimental findings in river morphodynamics, which suggest that alternating, point and mid-channel bars are related to fundamen-

tally different physical processes, which lead to different topographic expressions. Point bars are forced by a curved channel geometry (Blondeaux and Seminara, 1985), and alternate bars mostly develop as a result of a free instability mechanism of the riverbed topography (Tubino et al., 1999). In our work, when moving from morphologies 1 to 6, generated by a progressive widening under analogous hydraulic conditions (formative discharge, channel slope, sediment size) similar topographic differences are found. Future research shall concentrate on the relations between the topographic expressions of such bar units and the underlying morphodynamic processes.

4.2 Implications for Restoration of Hydropeaking Rivers

A central question related to "giving more room" to channelized rivers is whether morphological/structural measures alone would be effective when the river reach to be restored also suffers from hydrological alteration, and namely from hydropeaking (Fette et al., 2007). Harby and Noack (2013) suggest that "morphological restoration might be able to achieve the same mitigation effect than by adjusting hydro operations". Also Tuhtan et al. (2012) conclude that it may be possible to create fish shelters or, more in general to design instream refugia in addition to flow regime modifications. Paetzold et al. (2008) indicate that the combined conditions of hydropeaking inundation and gravel bar morphology are crucial for providing suitable habitats for the riparian arthropods, and that morphological river rehabilitation (e.g. channel widening) can benefit riparian arthropods, particularly in rivers that are affected by hydropeaking. Muhar et al. (2007) report that, contrary to expectations, little or no ecological improvements have been documented in some widened reaches subject to hydropeaking, indicating the need for a deeper quantitative investigation of hydropeaking-channel morphology interactions.

The mutual interplay between channel morphology and hydropeaking is agreed to represent a key phenomenon, but so far quantitative indications on its dynamics and eco-hydraulic effects have not been provided. In this respect, the proposed modeling approach can be used as a template for a quantitative analysis of the most effective tradeoffs between two different strategies aiming to achieve the same ecological target or between two different ecologi-

cal targets that pose contrasting hydro-morphological requirements. For instance the hydro-morphological alteration space originally proposed by Baumann et al. (2012) suggests how the same eco-hydraulic effect can often be obtained through both vertical and horizontal strategies. As an illustrative example, Figure 10c suggests that the same reduction in stranding risk corresponding to a wandering channel pattern ($W/W_0 = 5.33$) under the most intense hydropeaking scenario (A: $Q_{peak}/Q_{base} = 10$) can be obtained either by increasing the base flow from 5 to 20 m^3/s and keeping the same morphology or by reducing the active river corridor width of roughly 1.5 times (down to $W/W_0 \simeq 3.5$) without any variation of the hydropeaking intensity. Under the conditions of our simulations, both actions are predicted to achieve an increase of the area with low stranding risk from 47% to 70% of the total wetted area. Analogously, the same mitigation of sink area loss can be achieved in a channel with alternating bars by either a three-fold base flow increase or by widening the channel up to 2.5 times its initial width (Figure 10b). Also, the paradox posed by the contrasting trends of hydromorphological diversity (increases with morphological complexity) and of the percentage of stranding safe areas (which instead decreases with morphological complexity) can be given a quantitative answer. Channelization below morphological instability to occur should not be preferred to avoid stranding risk because of its overall poor eco-hydraulic functioning (see for example the overall score in Figure 11).

Besides providing a representation of the effects of base flow increase as a hydropeaking mitigation measure, moving along the vertical axis of the hydromorphological spaces like Figure 1 is also a way to account for the seasonal variability of the base flow typical of alpine rivers, where the combined effect of snowmelt and, in some cases of glacier melt, naturally increase base flow conditions even within hydropower-regulated river reaches. Our analysis suggests that the effects of base flow increase are morphology-dependent, because: (1) it maximizes the benefits for habitat diversity for transitional/wandering channel morphologies; (2) it minimizes the loss of invertebrate drift areas in channels with alternate bars and (3) it reduces stranding risk in braiding morphologies. Increasing base flow alone might be thought to lead to decreasing available habitats, but our work suggests that this effect is morphology-dependent and definitely not the case under transitional patterns. This reiterates the interaction with morphological miti-

gation especially when based on a design channel width for which a wandering morphology is expected.

A final consideration related to legal requirements on hydropeaking intensities can be made from looking at the three panels composing Figure 10. Regardless of the channel morphology, the worst ecological scenarios (red areas) appear to develop only for base to peak flow ratios smaller than 1:5, with larger ratios (smaller hydropeaking intensities) invariably producing milder effects for all the examined ERHPs. This quantitatively substantiates legal requirements on minimum base to peak flow ratios that are prescribed at 1:3 (Switzerland) or also 1:5 (Austria) (Hauer et al., 2014).

4.3 Applicability and Limitations of the Proposed Approach

Though our analysis has not been developed referring to actual specific cases, it is relevant to note that the hydromorphological conditions under which our modeling experiments have been designed are quite realistic. First, the considered ranges of widening ratios W/W_0 and of reach length (normalized with the channelized width W_0) are in good correspondence with those typical of river widening projects in alpine streams. Examples taken from selected river widening projects in the alpine region of Europe are reported in Table 2. It appears that the allowed width of the restored reach may be in the range of 1.5 to 6 times the channelized river width (vs. 1.3 to 10 of our study), while the typical length of widened reaches may range from 10 up to 100 times the same initial river width, an identical range to that employed in our analysis. Second, the considered range of hydropeaking intensities (1:3, 1:5, 1:10) is representative of many actual situations in Alpine streams (Hauer et al., 2014).

Another relevant factor for the applicability of our results to real hydropeaking streams is the simulated degree of inundation of the examined morphologies under base and peak flow conditions. Alternate bars ($W/W_0 = 2$) are overtopped by peak flows, which only partially inundate (70 to 80%) transitional and braiding morphologies. This is consistent with the few reported data for some Austrian rivers, indicating that gravel bars in the Alpine environment may only be overtopped in terms of hydropeaking, while the braided sections may not not fully

overtopped in terms of (theoretical) artificial fluctuating flows like in the Austrian Lech River (Auer, 2012).

The presented approach has therefore been developed referring to idealized though realistic combinations of hydropeaking waves of different intensities and of channel morphologies of varying complexity. In order to be applied to a given specific case the availability of the following data is required: the actual discharge time series of the reach, roughness and river bed topography data of the investigated reach. Channel morphology should be known at sufficient spatial resolution, i.e. a resolution which allows mapping the main two-dimensional riverbed features, like bars, bifurcations, secondary channels. Should only sparse cross-sections be available, a numerical morphodynamic model could be used to develop scenarios of the potential future morphological patterns of the reach. This might be used to choose the optimal channel width value when designing a local river widening project.

It is finally useful to review the main limitations of the present study. The chosen ERHPs are only some possible choices that cannot be considered exhaustively representative of the related eco-hydraulic process. For instance, the criterion used to quantify the variability in stranding risk (equation 3) is purely based on existing regulation, namely from the Swiss water protection guidelines (Baumann et al., 2012). Analogous plots could be derived using other specific regulations adopted in other countries, like Norway or Austria. In Norway a dewatering threshold has been suggested (Saltveit et al., 2001; Halleraker et al., 2003; Irvine et al., 2009; Tuhtan et al., 2012), which is based on the vertical flow level variation rather than on the wetted area variation. In Austria an analogous criterion (besides those on hydropeaking magnitude) of the Swiss one is used though with a 20% rather than an 30% threshold. More specific criteria are needed to predict more in detail the actual response of the eco-hydraulic process to different morphologies under hydropeaking. For instance in the case of stranding, Hauer et al. (2014) account for the relevant role of the substrate size, which is not considered in this analysis. Moreover, the worst possible scenario of ramping rate has been considered, by assuming an instantaneous shift from base to peak flow and viceversa. Therefore the stranding risk maps (Figure 10c) have to be viewed as an upper limit for that ERHP. More in general, the present

approach is not able to predict the actual biological response of a reach to hydropeaking, but only its response in terms of the physical conditions that can be of relevance for a specific biotic element.

On the other hand, the potential of the proposed approach also lies in its capability to incorporate other Ecologically-Relevant Hydraulic Parameters that have not been examined within this work like, e.g. the physical habitat availability of a target species, which can be obtained by integrating the outcomes of the hydraulic model with the specific hydraulic preference information or habitat rating curves. This would lead to a tailored version of the hydro-morphological alteration space of Figure 1 for the design case.

Finally it must be noted that the assumed biunique relation between channel widening (i.e. the parameter W/W_0) and the developed riverbed morphology holds only when adequate sources of sediment supply are connected with the target river reach; therefore an implicit assumption of our study has been that of enough availability of upstream sediment supply, which may not always be the same in regulated alpine streams.

5 Conclusions

The present work consists of a first quantitative attempt to investigate the eco-hydraulic response of river reaches with different channel morphologies to hydropeaking waves. It is based on a hydraulic modeling approach and it focuses on three eco-hydraulic phenomena with well known relevance under hydropeaking conditions: habitat diversity, macroinvertebrate drift and fish stranding. A series of 18 combinations of 3 hydropeaking waves having different intensity (ratio Q_{peak}/Q_{base}) with 6 channel morphologies of increasing complexity (from nearly flat bed to alternate bars, wandering and braiding) are investigated in terms of Ecologically Relevant Hydraulic Parameters (ERHPs) chosen to measure the target eco-hydraulic phenomena. Under the assumptions and simplifications described in Section 2 we performed steady hydraulic simulations via a 2-D numerical model for both base and peak flow conditions for each of the 18 combinations, which can be viewed as realistic replicates of actual scenarios occurring in

Alpine region.

Non-linear trends are predicted for the chosen ERHPs with both hydropeaking intensity and morphological complexity. Habitat diversity and fish stranding risk are mostly controlled by channel morphology and show contrasting behaviours with increasing morphological complexity. Braided reaches are the most resilient to hydropeaking offering the highest habitat diversity, very limited base-to-peak loss of sink areas of drifting invertebrates and also of habitat diversity, while alternate bars are extremely sensitive environments to drift and offer safer regions from stranding. Transitional morphologies between single- and multi-thread, which have increasingly replaced formerly braided reaches in the regulated river landscape, offer the best eco-hydraulic tradeoffs. The proposed approach can be applied to a specific case to support the choice of the most effective river restoration strategy leading to the optimal eco-hydraulic conditions for the ecological targets of primary interest.

Ecological effects are the results of complex interactions of several parameters, thus simplifications had to be introduced aiming at model and quantify some ERHPs. Being aware of the other relevant parameters not considered here, we are confident that extending the presented approach to other ERHPs (for example considering the role of discharge rate of change) can usefully increase current understanding of ecological implications of hydropeaking.

Acknowledgements

The present work has been partially supported through a grant provided by the APRIE (Agenzia per le Risorse Idriche e l'Energia) of the Provincia Autonoma di Trento. Laboratory bathymetries have been kindly provided from the doctoral thesis of Garcia Lugo G. Alejandra (*Braided rivers: an exploratory study combining flume experiments and the analysis of remotely-sensed data*. Queen Mary University of London, 2014).

References

Auer, H. (2012). Flussmorphologische Grundlagenuntersuchungen am Lech zur Bewertung des Schwalleinflusses bei unterschiedlichen Flusstypen. Master's thesis, University of Natural Resources and Life Sciences, Vienna.

Baumann, P. , Kirchhofer, A. , and Schälchli, U. (2012). Risanamento deflussi discontinui - Pianificazione strategica. Un modulo dell'aiuto all'esecuzione Rinaturazione delle acque. Technical report, Ufficio federale dell'ambiente, Bern, CH.

Bertoldi, W. , Gurnell, A. , Surian, N. , Tockner, K. , Zanoni, L. , Ziliani, L. , and Zolezzi, G. (2009). Understanding reference processes: Linkages between river flows, sediment dynamics and vegetated landforms along the Tagliamento River, Italy. *River Research and Applications*, 25(February):501–516. doi: 10.1002/rra.1233.

Blondeaux, P. and Seminara, G. (1985). A unified bar-bend theory of river meanders. *Journal of Fluid Mechanics*, 157:449. doi: 10.1017/S0022112085002440.

Bruno, M. C. , Maiolini, B. , Carolli, M. , and Silveri, L. (2010). Short time-scale impacts of hydropeaking on benthic invertebrates in an Alpine stream (Trentino, Italy). *Limnologica - Ecology and Management of Inland Waters*, 40(4):281–290. doi: 10.1016/j.limno.2009.11.012.

Bruno, M. C. , Siviglia, A. , Carolli, M. , and Maiolini, B. (2013). Multiple drift responses of benthic invertebrates to interacting hydropeaking and thermopeaking waves. *Ecohydrology*, 6(4):511–522. doi: 10.1002/eco.1275.

Campana, D. , Marchese, E. , Theule, J. I. , and Comiti, F. (2014). Geomorphology Channel degradation and restoration of an Alpine river and related morphological changes. *Geomorphology*, 221:230 241. doi: 10.1016/j.geomorph.2014.06.016.

Casas-Mulet, R. , Alfredsen, K. , Boissy, T. , Sundt, H. , and Rüther, N. (2014a). Performance

of a one-dimensional hydraulic model for the calculation of stranding areas in hydropeaking rivers. *River Research and Applications*, pages n/a–n/a. doi: 10.1002/rra.2734.

Casas-Mulet, R. , Saltveit, S. J. , and Alfredsen, K. (2014b). The survival of atlantic salmon (Salmo salar) eggs during dewatering in a river subjected to hydropeaking. *River Research and Applications*, 7:n/a–n/a. doi: 10.1002/rra.2827.

Céréghino, R. , Legalle, M. , and Lavandier, P. (2004). Drift and benthic population structure of the mayfly Rhithrogena semicolorata (Heptageniidae) under natural and hydropeaking conditions. *Hydrobiologia*, 519(1-3):127–133. doi: 10.1023/B:HYDR.0000026499.53979.69.

Charmasson, J. and Zinke, P. (2011). Mitigation Measures Against Hydropeaking Effects. Technical report, SINTEF Energy Research.

Crosato, A. and Mosselman, E. (2009). Simple physics-based predictor for the number of river bars and the transition between meandering and braiding. *Water Resources Research*, 45(3): n/a–n/a. doi: 10.1029/2008WR007242.

Elosegi, A. , Díez, J. , and Mutz, M. (2010). Effects of hydromorphological integrity on biodiversity and functioning of river ecosystems. *Hydrobiologia*, 657(1):199–215. doi: 10.1007/s10750-009-0083-4.

Fette, M. , Weber, C. , Peter, a. , and Wehrli, B. (2007). Hydropower production and river rehabilitation: A case study on an alpine river. *Environmental Modeling & Assessment*, 12 (4):257–267. doi: 10.1007/s10666-006-9061-7.

Formann, E. , Habersack, H. , and Schober, S. (2007). Morphodynamic river processes and techniques for assessment of channel evolution in Alpine gravel bed rivers. *Geomorphology*, 90(3-4):340–355. doi: 10.1016/j.geomorph.2006.10.029.

Garcia Lugo, A. G. , Bertoldi, W. , and Gurnell, A. (2013). Flume experiments to investigate multi-thread channel development under controlled conditions. In *British Society for Geomorphology Annual Meeting*.

Gostner, W. , Alp, M. , Schleiss, A. J. , and Robinson, C. T. (2013a). The hydro-morphological index of diversity: a tool for describing habitat heterogeneity in river engineering projects. *Hydrobiologia*, 712(1):43–60. doi: 10.1007/s10750-012-1288-5.

Gostner, W. , Parasiewicz, P. , and Schleiss, a. J. (2013b). A case study on spatial and temporal hydraulic variability in an alpine gravel-bed stream based on the hydromorphological index of diversity. *Ecohydrology*, 6(4):652–667. doi: 10.1002/eco.1349.

Habersack, H. M. and Piegay, H. (2007). Challenges in river restoration in the Alps and their sorrounding areas. In Habersack, Helmut; Piégay, Hervé; Rinaldi, M. , editor, *Gravel Bed Rivers 6: From Process Understanding to River Restoration*, pages 703–737. Elsevier.

Halleraker, J. H. , Saltveit, S. J. , Harby, A. , Arnekleiv, J. V. , Fjeldstad, H.-P. H.-P. , and Kohler, B. (2003). Factors influencing stranding of wild juvenile brown trout (Salmo trutta) during rapid and frequent flow decreases in an artificial stream. *River Research and Applications*, 19(5-6):589–603. doi: 10.1002/rra.752.

Harby, A. and Noack, M. (2013). *Ecohydraulics*. John Wiley & Sons. doi: 10.1002/9781118526576.ch19.

Hauer, C. , Unfer, G. , Graf, W. , Leitner, P. , Zeiringer, B. , and Habersack, H. (2012). Hydro-morphologically related variance in benthic drift and its importance for numerical habitat modelling. *Hydrobiologia*, 683(1):83–108. doi: 10.1007/s10750-011-0942-7.

Hauer, C. , Schober, B. , and Habersack, H. (2013). Impact analysis of river morphology and roughness variability on hydropeaking based on numerical modelling. *Hydrological Processes*, 27(15):2209–2224. doi: 10.1002/hyp.9519.

Hauer, C. , Unfer, G. , Holzapfel, P. , Haimann, M. , and Habersack, H. (2014). Impact of channel bar form and grain size variability on estimated stranding risk of juvenile brown trout during hydropeaking. *Earth Surface Processes and Landforms*, 1641(March):n/a–n/a. doi: 10.1002/esp.3552.

Holland, S. P. and Mansur, E. T. (2008). Is Real-Time Pricing Green? The Environmental Impacts of Electricity Demand Variance. *Review of Economics and Statistics*, 90(3):550–561. doi: 10.1162/rest.90.3.550.

Irvine, R. L. , Oussoren, T. , Baxter, J. S. , and Schmidt, D. C. (2009). The effects of flow reduction rates on fish stranding in British Columbia, Canada. *River Research and Applications*, 25(4):405–415. doi: 10.1002/rra.1172.

Jones, N. E. (2014). The dual nature of hydropeaking rivers: is ecopeaking possible? *River Research and Applications*, 30(4):521–526. doi: 10.1002/rra.2653.

Meile, T. , Boillat, J.-L. , and Schleiss, A. (2008). Reduction of Hydropeaking in Rivers by Bank Macro Rroughness. *WASSERWIRTSCHAFT*, 98(12):18–24.

Muhar, S. , Jungwirth, M. , Wiesner, C. , Poppe, M. , Schmutz, S. , Hohennsinner, S. , and Habersack, H. (2007). Restoring riverine landscapes at Drau River: successes and deficits in the context of ecological integrity. In *Gravel-Bed Rivers VI: From Process Understanding to River Restoration*, volume 2025, pages 779–803. doi: 10.1016/S0928-2025(07)11164-0.

Nagrodski, A. , Raby, G. D. , Hasler, C. T. , Taylor, M. K. , and Cooke, S. J. (2012). Fish stranding in freshwater systems: sources, consequences, and mitigation. *Journal of environmental management*, 103:133–41. doi: 10.1016/j.jenvman.2012.03.007.

Paetzold, A. , Yoshimura, C. , and Tockner, K. (2008). Riparian arthropod responses to flow regulation and river channelization. *Journal of Applied Ecology*, 45:894–903. doi: 10.1111/j.1365-2664.2008.01463.x.

Person, E. , Bieri, M. , Peter, A. , and Schleiss, A. J. (2013). Mitigation measures for fish habitat improvement in Alpine rivers affected by hydropower operations. *Ecohydrology*, pages n/a–n/a. doi: 10.1002/eco.1380.

Rohde, S. , Schütz, M. , Kienast, F. , and Englmaier, P. (2005). River widening: an approach

to restoring riparian habitats and plant species. *River Research and Applications*, 21(10): 1075–1094. doi: 10.1002/rra.870.

Rohde, S. , Hostmann, M. , Peter, A. , and Ewald, K. (2006). Room for rivers: An integrative search strategy for floodplain restoration. *Landscape and Urban Planning*, 78(1-2):50–70. doi: 10.1016/j.landurbplan.2005.05.006.

Saltveit, S. J. , Halleraker, J. H. , Arnekleiv, J. V. , and Harby, A. (2001). Field experiments on stranding in juvenile atlantic salmon (\textit{Salmo salar}) and brown trout (\textit{Salmo trutta}) during rapid flow decreases caused by hydropeaking. *Regul. River*, 17(4-5):609–622. doi: 10.1002/rrr.652.

Siviglia, A. , Repetto, R. , Zolezzi, G. , and Tubino, M. (2008). River bed evolution due to channel expansion: general behaviour and application to a case study (Kugart River, Kyrgyz Republic). *River Research and Applications*, 24(9):1271–1287. doi: 10.1002/rra.1095.

Siviglia, A. , Stecca, G. , Vanzo, D. , Zolezzi, G. , Toro, E. F. , and Tubino, M. (2013). Numerical modelling of two-dimensional morphodynamics with applications to river bars and bifurcations. *Advances in Water Resources*, 52:243–260. doi: 10.1016/j.advwatres.2012.11.010.

Surian, N. and Rinaldi, M. (2003). Morphological response to river engineering and management in alluvial channels in Italy. *Geomorphology*, 50(4):307–326. doi: 10.1016/S0169-555X(02)00219-2.

Swiss Federal Office of Energy (2013). Energieperspektiven 2050: Zusammenfassung. Technical report, Swiss Federal Office of Energy.

Trentini, G. , Monaci, M. , Goltera, A. , Comiti, F. , Gallmetzer, W. , and Mazzorana, B. , editors (2012). *Riqualificazione del Rio Mareta: pianificazione e prime fasi di attuazione*. bu.press, Bolzano.

Tubino, M. , Repetto, R. , and Zolezzi, G. (1999). Free bars in rivers. *Journal of Hydraulic Research*, 37(6):759–775. doi: 10.1080/00221689909498510.

Tuhtan, J. a. , Noack, M. , and Wieprecht, S. (2012). Estimating stranding risk due to hydropeaking for juvenile European grayling considering river morphology. *KSCE Journal of Civil Engineering*, 16(2):197–206. doi: 10.1007/s12205-012-0002-5.

Vehanen, T. , Jurvelius, J. , and Lahti, M. (2005). Habitat utilisation by fish community in a short-term regulated river reservoir. *Hydrobiologia*, 545(1):257–270. doi: 10.1007/s10750-005-3318-z.

Young, P. S. , Cech, J. J. , and Thompson, L. C. (2011). Hydropower-related pulsed-flow impacts on stream fishes: a brief review, conceptual model, knowledge gaps, and research needs. *Reviews in Fish Biology and Fisheries*, 21(4):713–731. doi: 10.1007/s11160-011-9211-0.

Table 1: Hydro-morphological configurations: three different hydropeaking patterns (column A, B and C of upper panel) characterized by same electricity production Q_{prod} but different ratio of Q_{peak}/Q_{base}. Six self-formed morphologies (row 1 to 6 of lower panel) upscaled from experimental runs; widening ratio refers to the first morphology of 15m width.

Prod. pattern	A	B	C
$Q_{prod}\,[m^3/s]$	45	45	45
$Q_{peak}\,[m^3/s]$	50	55	65
$Q_{base}\,[m^3/s]$	5	10	20
Q_{peak}/Q_{base}	10	5.5	3.25

Morphology number	**Total width** $[m]$	**Equilibrium pattern**	**Widening ratio** W/W_0
1	15	flat bed	1
2	20	alternate bars	1.33
3	30	alternate bars	2
4	80	wandering	5.33
5	100	braiding	6.66
6	150	braiding	10

Table 2: Some examples of European river widening projects.

River - Country	**Widening ratio**	**Channelized width** [m]	**Widening length** [m]	**Reference**
Rio Mareta - I	2-3	20	2000	Trentini et al. (2012)
Aurino - I	2-3	50	1000+800	Campana et al. (2014)
Thur - CH	2-3	50	1500	www.rivermanagement.ch
Kander - CH	6	20	500	www.rivermanagement.ch
Mur - A	2-3	70	2500	Gosdorf Project - Mur River
Drau - A	1.5-2	50	450	LIFE-Project Upper Drau River
Isar - D	2	50	9000	www.rivermanagement.ch

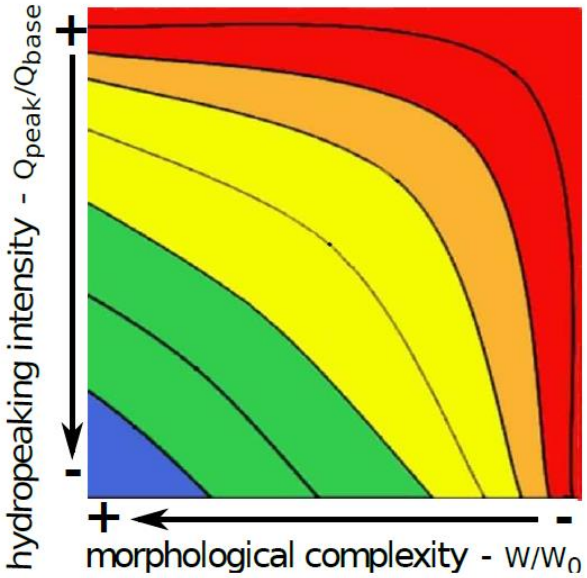

Figure 1: Hydro-morphological alteration space: qualitative ecological response to interaction between hydropeaking pressure (vertical axis) and morphological complexity (horizontal axis) of receiving river reach, inspired by Baumann et al., 2012. Downward vertical shifts in the plot correspond to reducing hydropeaking intensities, while horizontal shifts correspond to increasing morphological complexity (right to left). Red and blue regions represent the expected worst and best state from ecological point of view, respectively.

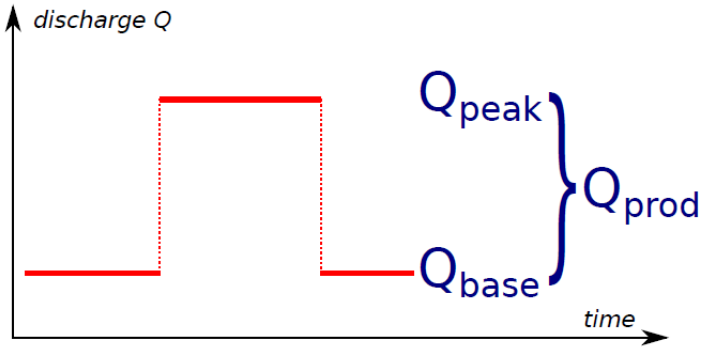

Figure 2: The hydropeaking event is schematized as a rectangular wave, varying from a base (Q_{base}) and a peak (Q_{peak}) discharge.

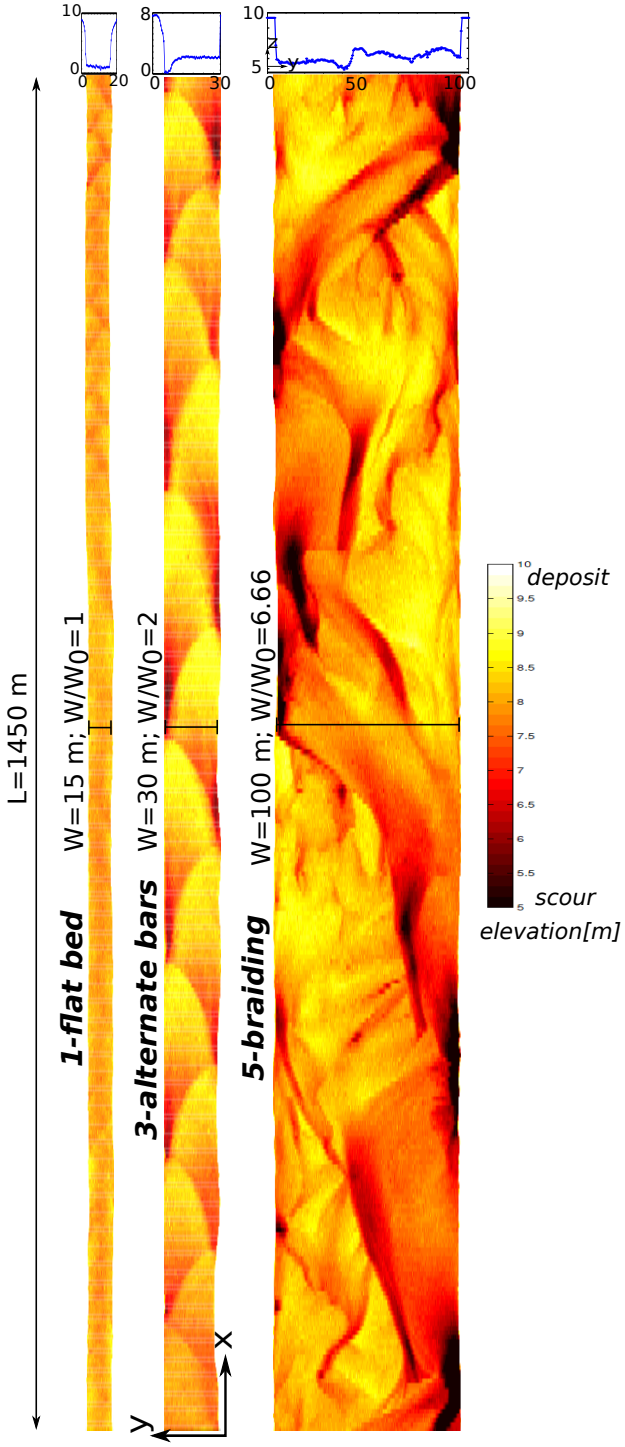

Figure 3: Example of (y-z) cross section (on the top) and (x-y) planar view for three different morphologies: flat bed (1), alternate bars (3) and braiding network (5), with a widening ratio W/W_0 of 1, 2 and 6.66 respectively.

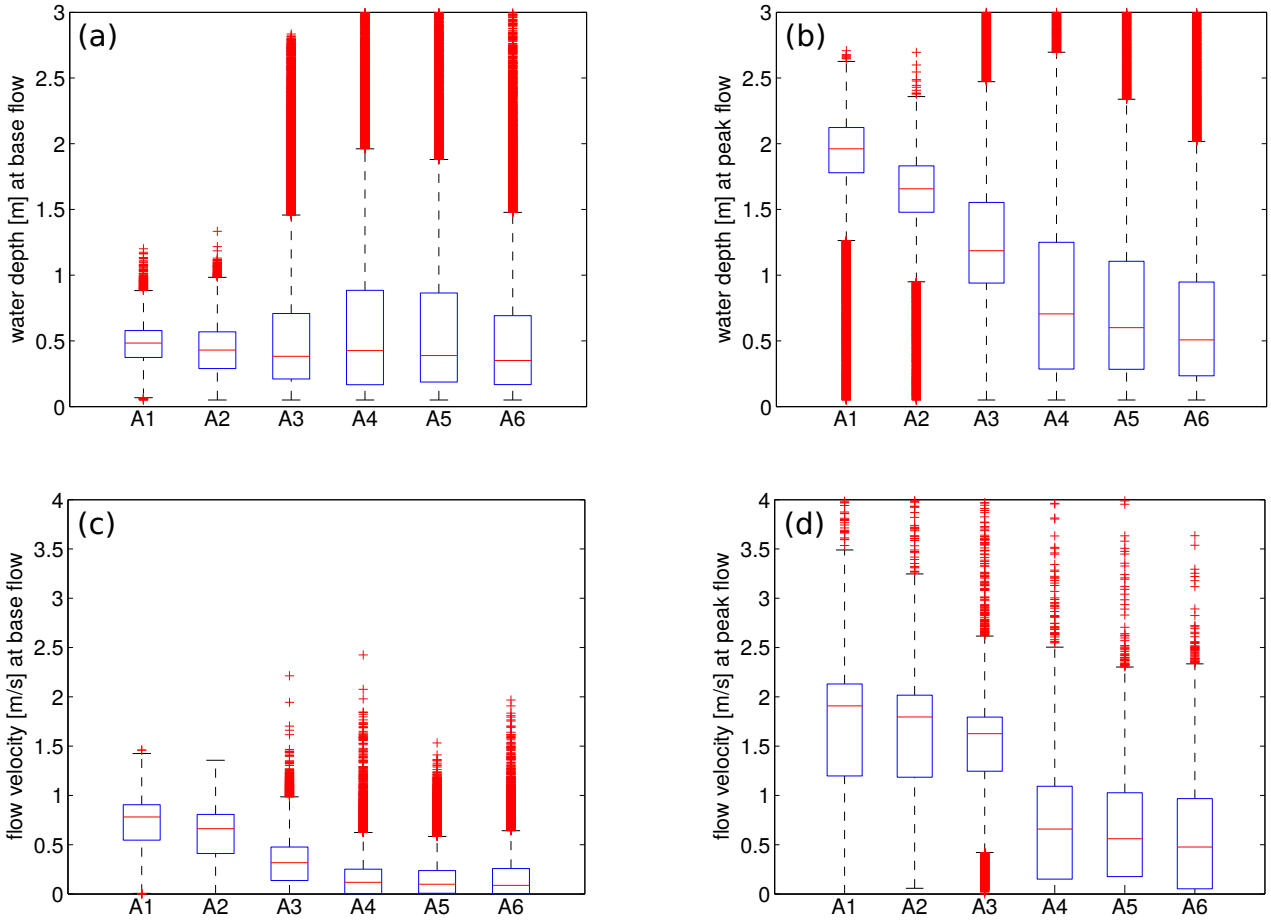

Figure 4: Box and whiskers plot for the distributions of water depth (panels a and b) and of longitudinal flow velocity (panels c and d) of the considered six morphologies (from 1 to 6) for the production pattern A, both for base (panels a and c) and peak flow conditions (panels b and d).

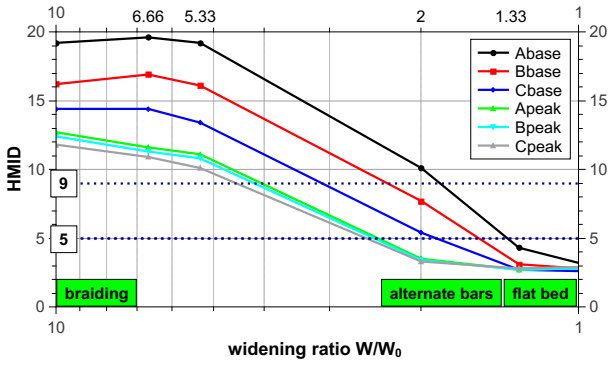

Figure 5: HMID index versus six widening ratios. Series represent the different release patterns (A,B and C) both for peak and base flow; dotted lines represent category thresholds proposed by Gostner et al. (2013a).

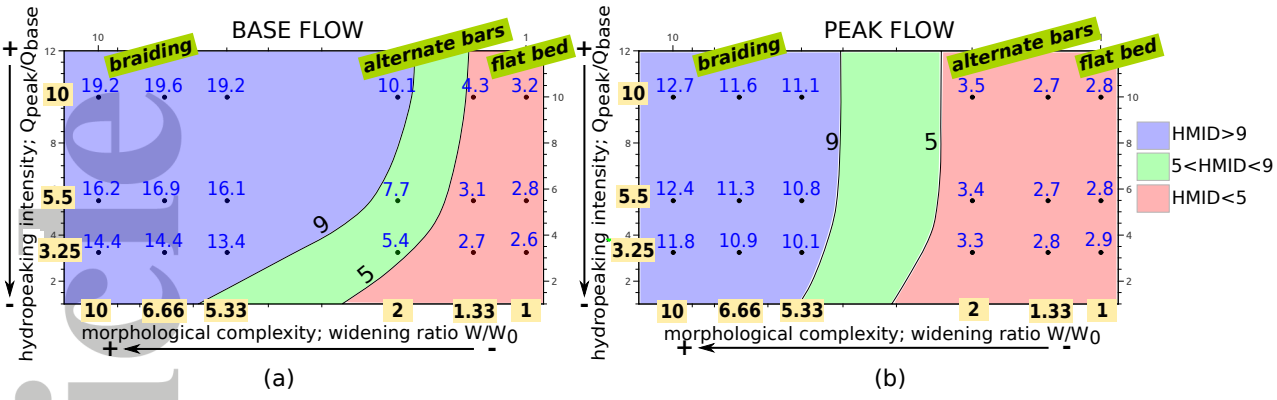

Figure 6: Hydro-morphological alteration space of HMID for base (panel a) and peak flow (panel b). Blue regions represent configuration with $HMID > 9$ (morphologically natural), red regions with $HMID < 5$ (morphologically heavily altered) while intermediate green regions represent transitional configurations. Black dots correspond to configurations of the numerical runs while blue labels are the obtained HMID values.

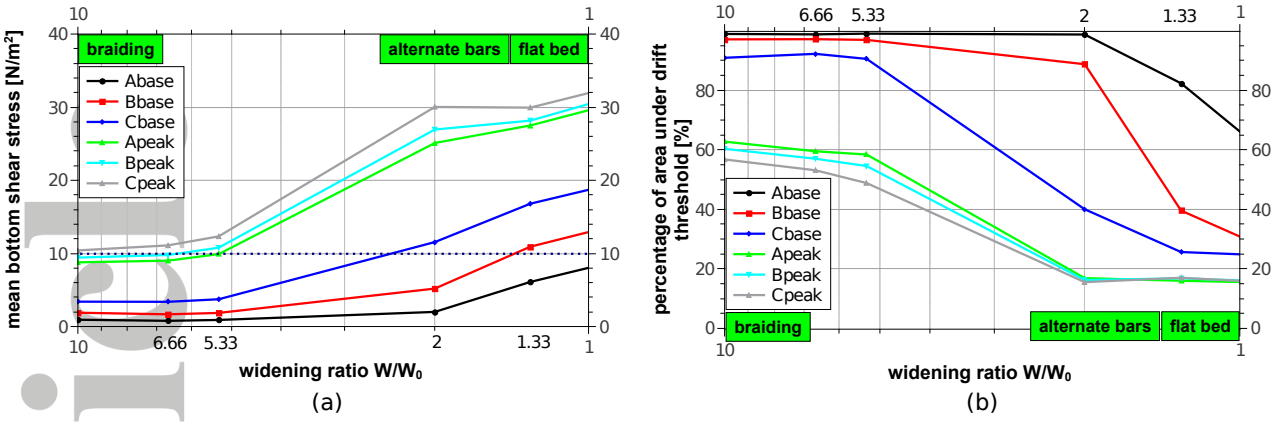

Figure 7: Panel a: mean of the bottom shear stress versus six widening ratios corresponding to the different morphologies; the dotted line denotes the drift threshold $\tau_{drift} = 10\ N/m^2$ (Hauer et al., 2012). Panel b: percentage of area with bottom shear stress lower than the drift threshold τ_{drift} versus six widening ratios. In both panels the series represent the different release patterns (A,B and C) both for peak and base flow.

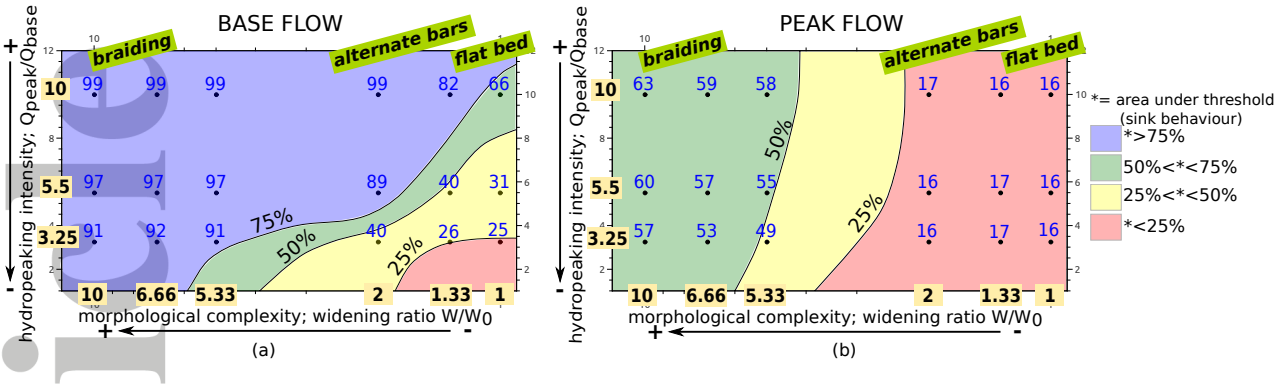

Figure 8: Hydro-morphological alteration space of macroinvertebrate drift for base (panel a) and peak flow (panel b). Blue regions represent configurations with dominant (more then 75%) settling of macroinvertrebrate communities (sink areas) while red ones represent scenarios dominated by macroinvertebrate drifting (source areas). Black dots correspond to configurations of the numerical runs while blue labels are the percentages of area with sink behaviour.

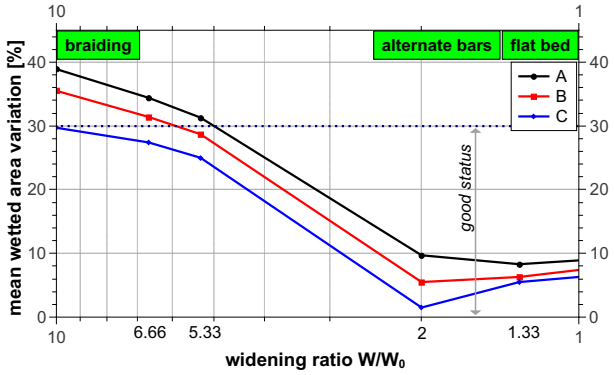

Figure 9: Mean wetted area variation versus six widening ratios; dotted line is the threshold proposed in Swiss protocol (Baumann et al., 2012) to discriminate the low stranding risk (good status).

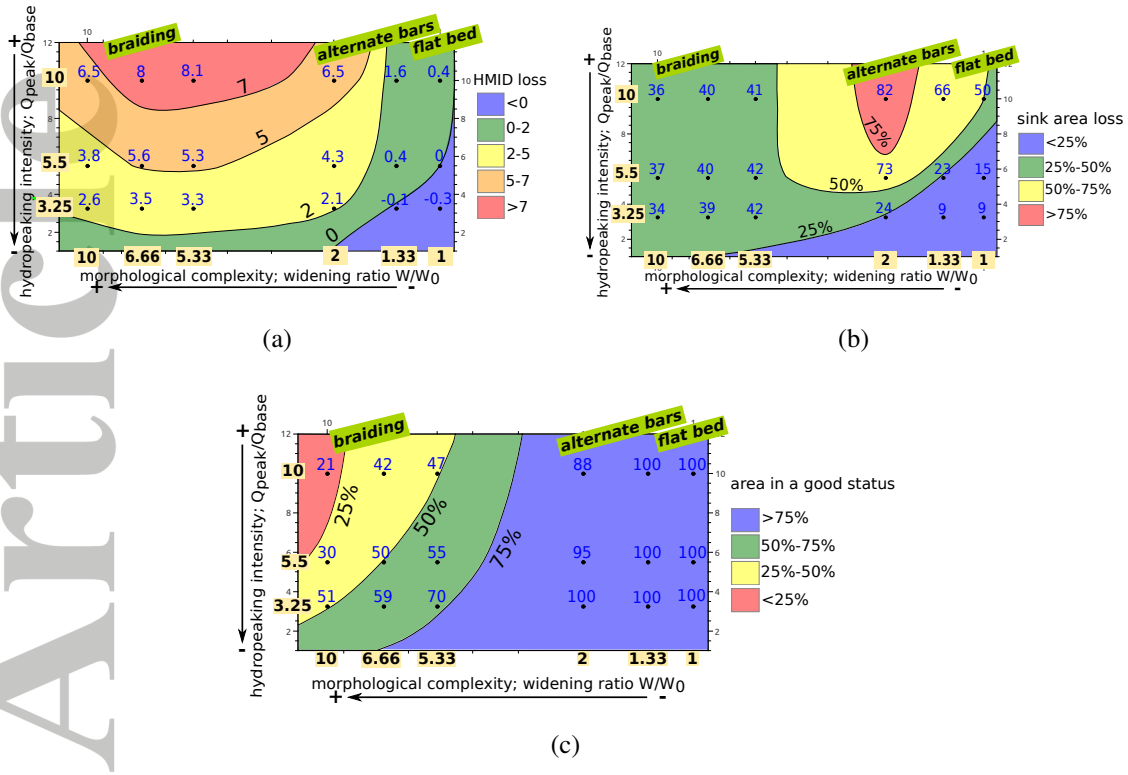

(a) (b)

(c)

Figure 10: Hydro-morphological alteration space of ERHPs variation passing from Q_{base} to Q_{peak}: (a) variation of HMID index; (b) variation of area with sink behaviour; (c) percentage of area with low risk of stranding.

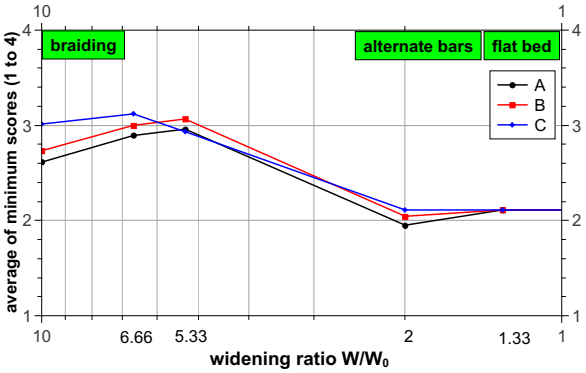

Figure 11: Classes of hydro-morphological quality for the three ERHPs under repeated hydropeaking.